Dynamics of Solvent and Rotational Relaxation of Coumarin 153 in a Room Temperature Ionic Liquid, 1-Butyl-3-methylimidazolium Octyl Sulfate, Forming Micellar Structure

Debabrata Seth, Souravi Sarkar, and Nilmoni Sarkar*

Department of Chemistry, Indian Institute of Technology, Kharagpur 721 302, WB, India

Received November 17, 2007. Revised Manuscript Received April 22, 2008

The solvent and rotational relaxation of Coumarin 153 (C-153) was investigated by picosecond time-resolved fluorescence spectroscopy in a room temperature ionic liquid (RTIL), 1-butyl-3-methylimidazolium octyl sulfate ($[C_4mim][C_8SO_4]$). This is a typical RTIL, which form micellar structure above certain concentration of the RTIL (0.031 M). Dynamic light scattering (DLS) measurements show that the average hydrodynamic diameter (D_h) of a $[C_4mim][C_8SO_4]$−water micelle is 2.8 (±0.2) nm. Both the solvent and rotational relaxation of C-153 are retarded in this micelle compared to the solvation time of a similar type of dye in neat water. However, the solvent relaxation in this ionic liquid surfactant is different from that of a conventional ionic surfactant. The slow component of the solvation dynamics in $C_8H_{17}SO_4Na$ or TX-100 micelle is on the nanoseconds time scale, whereas in $[C_4mim][C_8SO_4]$ micelle the same component is on the subnanoseconds time scale. The different molecular motions with different time scale is the main reason behind this difference in the solvation time in micelles composed of RTIL with other conventional micelles.

1. Introduction

Room temperature ionic liquids (RTILs) exhibit interesting and unusual physical properties, such as low vapor pressure, high thermal stability, wide liquidous temperature range, and wide electrochemical windows. These unique features make them as alternative green substitute for volatile organic compounds (VOCs). RTILs are composed solely of ions. Cations of RTILs are generally organic and anions are generally inorganic in nature. By proper selection of cation and anion several RTIL can be prepared with desired properties.

Due to their unusual properties, RTILs have been used in many chemical reactions.[1,2] The most widely used RTILs generally contain *N*,*N*-dialkylimidazolium cations and inorganic anions like PF_6^-, BF_4^-, and $[(CF_3SO_2)_2N]^-$. In general, most of the anions of RTILs contain fluorine molecule. Sometimes these fluorine-containing anions such as PF_6^- hydrolyzed in the presence of water to produce volatile, harmful, and corrosive HF, POF_3, etc.[3,4] Due to this drawback, some alternative anions has been introduced. The RTILs based on $CF_3SO_3^-$, $(CF_3SO_3)_2N^-$, etc. anions are relatively inert to hydrolysis because the C−F bond is inert to hydrolysis. Some alkylsulfate anions containing RTILs have been introduced that are biodegradable and likely to be nontoxic.[5]

In recent years, there is a tremendous interest to investigate different types of physical and chemical properties of RTILs. Several physical, photophysical, and ultrafast spectroscopic studies and also several theoretical studies investigated these RTILs.[6–30] The nature of solvation in neat RTILs was investigated both experimentally and theoretically.[9–25] The effect of micromolar addition of polar solvent on the solvation dynamics of RTILs was also investigated.[26,27] Recently, RTILs containing micelles and microemulsions have received much attention.

* Corresponding author. Fax: 91-3222-255303. E-mail: nilmoni@chem.iitkgp.ernet.in.

(1) Welton, T.; Wasserscheid, P. (Eds.) *Ionic Liquids in Synthesis*; Wiley-VCH, Weinheim, 2002.
(2) (a) Parvulescu, V. I.; Hardacre, C. *Chem. Rev.* **2007**, *107*, 2615. (b) Chowdhury, S.; Mohan, R. S.; Scott, J. L. *Tetrahedron* **2007**, *63*, 2363. (c) Plechkova, N. V.; Seddon, K. R. *Chem. Soc. Rev.* **2008**, *37*, 123. (d) Dupont, J.; de Souza, R. F.; Suarez, P. A. Z. *Chem. Rev.* **2002**, *102*, 3667.
(3) Swatloski, R. P.; Holbrey, J. D.; Rogers, R. D. *Green Chem.* **2003**, *5*, 361.
(4) Baker, G. A.; Baker, S. N. *Aust. J. Chem.* **2005**, *58*, 174.
(5) Wasserscheid, P.; Van Hal, R.; Bösmann, A. *Green Chem.* **2002**, *4*, 400.
(6) Aki, S. N. V. K.; Brennecke, J. F.; Samanta, A. *Chem. Commun.* **2001**, 413.
(7) Muldoon, M. J.; Gordon, C. M.; Dunkin, I. R. *J. Chem. Soc., Perkin Trans. 2* **2001**, 33.
(8) Reichardt, C. *Green Chem.* **2005**, *7*, 339.
(9) Karmakar, R.; Samanta, A. *J. Phys. Chem. A* **2002**, *106*, 4447.
(10) Karmakar, R.; Samanta, A. *J. Phys. Chem. A* **2002**, *106*, 6670.
(11) Karmakar, R.; Samanta, A. *J. Phys. Chem. A* **2003**, *107*, 7340.
(12) Saha, S.; Mandal, P. K.; Samanta, A. *Phys. Chem. Chem. Phys.* **2004**, *6*, 3106.
(13) Mandal, P. K.; Samanta, A. *J. Phys. Chem. B* **2005**, *109*, 15172.
(14) Samanta, A. *J. Phys. Chem. B* **2006**, *110*, 13704.
(15) Paul, A.; Samanta, A. *J. Phys. Chem. B* **2007**, *111*, 4724.
(16) Ingram, J. A.; Moog, R. S.; Ito, N.; Biswas, R.; Maroncelli, M. *J. Phys. Chem. B* **2003**, *107*, 5926.
(17) Ito, N.; Arzhantsev, S.; Heitz, M.; Maroncelli, M. *J. Phys. Chem. B* **2004**, *108*, 5771.
(18) Arzhantsev, S.; Ito, N.; Heitz, M.; Maroncelli, M. *Chem. Phys. Lett.* **2003**, *381*, 278.
(19) Ito, N.; Arzhantsev, S.; Maroncelli, M. *Chem. Phys. Lett.* **2004**, *396*, 83.
(20) Arzhantsev, S.; Jin, H.; Baker, G. A.; Maroncelli, M. *J. Phys. Chem. B* **2007**, *111*, 4978.
(21) Lang, B.; Angulo, G.; Vauthey, E. *J. Phys. Chem. A* **2006**, *110*, 7028.
(22) (a) Chowdhury, P. K.; Halder, M.; Sanders, L.; Calhoun, T.; Anderson, J. L.; Armstrong, D. W.; Song, X.; Petrich, J. W. *J. Phys. Chem. B* **2004**, *108*, 10245. (b) Mukherjee, P.; Crank, J. A.; Halder, M.; Armstrong, D. W.; Petrich, J. W. *J. Phys. Chem. A* **2006**, *110*, 10725. (c) Mukherjee, P.; Crank, J. A.; Sharma, P. S.; Wijeratne, A. B.; Adhikary, R.; Bose, S.; Armstrong, D. W.; Petrich, J. W. *J. Chem. Phys. B* **2008**, *112*(11), 3390.
(23) Baker, S. N.; Baker, G. A.; Munson, C. A.; Chen, F.; Bukowski, E. J.; Cartwright, A. N.; Bright, F. V. *Ind. Eng. Chem. Res.* **2003**, *42*, 6457.
(24) (a) Kobark, M. N. *J. Chem. Phys.* **2006**, *125*, 064502/1. (b) Shim, Y.; Choi, M. Y.; Kim, H. J. *J. Chem. Phys.* **2006**, *122*, 044511/1.
(25) (a) Hu, Z.; Margulis, C. J. *Acc. Chem. Res.* **2007**, *40*, 1097. (b) Shim, Y.; Jeong, D.; Manjari, S.; Choi, M. Y.; Kim, H. J. *Acc. Chem. Res.* **2007**, *40*, 1130. (c) Castner, E. W., Jr.; Wishart, J. F.; Shirota, H. *Acc. Chem. Res.* **2007**, *40*, 1217.
(26) Chakrabarty, D.; Chakraborty, A.; Seth, D.; Hazra, P.; Sarkar, N. *Chem. Phys. Lett.* **2004**, *397*, 469.
(27) Chakrabarty, D.; Chakraborty, A.; Seth, D.; Sarkar, N. *J. Phys. Chem. A* **2005**, *109*, 1764.
(28) Hu, Z.; Margulis, C. J. *Proc. Natl. Acad. Sci., U.S.A.* **2006**, *103*, 831.
(29) Shirota, H.; Funston, A. M.; Wishart, J. F.; Castner, E. W., Jr *J. Chem. Phys.* **2005**, *122*, 184512.
(30) Shirota, H.; Castner, E. W., Jr. *J. Phys. Chem. B* **2005**, *109*, 21576.

10.1021/la800813u CCC: $40.75
Published on Web 06/14/2008

Several groups prepared and characterized RTILs containing micelles and microemulsions.[31–36] The self-aggregation behavior of RTILs in aqueous solution has recently attracted much attention[36] due to structural similarities of RTILs with ionic surfactants. The surface activity of the long-chain imidazolium RTILs is superior to conventional ionic surfactants with the same hydrocarbon chain length.[36k] Recently, Miskolczy et al.[36a] showed that a RTIL can form micelles in aqueous solution. They used 1-butyl-3-methylimidazolium octyl sulfate ($[C_4mim][C_8SO_4]$) as the RTIL. The critical micellar concentration (cmc) of this RTIL-containing micelle is 0.031 M. This alkyl sulfate based, nonhalogenated RTIL is cheaper because it is derived from inexpensive chemicals.[37a] The physical properties of $[C_4mim][C_8SO_4]$ were studied.[37b] Quantum calculations[37b] on neat $[C_4mim][C_8SO_4]$ show strong hydrogen bonding between ion pair leads to a fluid structure. These new classes of amphiphiles based on RTILs are used as templates for preparation of silicate thin films.[38] The major limitation of RTILs is their inability to dissolve a number of chemicals, although the properties of RTILs can be tuned. To overcome this problem, RTILs were used to form micelles or microemulsions in water, and the solute molecules can be solubilized in the dispersed water phase.[33–36] By fine-tuning the hydrophobicity of the RTILs, one can modify the major characteristics such as the cmc, aggregation number, and micropolarity of the micelles dispersed in water. In this paper, we have investigated the solvent and rotational relaxation of C-153 in a micelle composed of an RTIL. The structures of C-153 and $[C_4mim][C_8SO_4]$ are shown in Scheme 1. It is interesting to investigate the solvent and rotational relaxation in this micelle composed of an RTIL. Moreover, we would like to compare the dynamics of solvent and rotational relaxation in this micelle with other conventional micelles.[42,47,48] The basic aim of this work is to find the uniqueness of the nature of RTIL surfactant in comparison with typical anionic surfactants. Moreover, this RTIL can form micelle above a certain concentration, which is not common for other RTILs.

Scheme 1. Structures of 1-Butyl-3-methylimidazolium Octyl Sulfate ($[C_4mim][C_8SO_4]$) and C-153

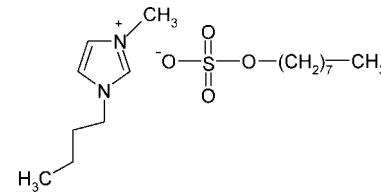

1-Butyl-3-methylimidazolium Octyl Sulfate

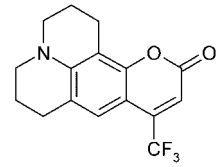

Coumarin 153 (C-153)

2. Experimental Section

C-153 (laser grade, Exciton) was used as received. $[C_4mim][C_8SO_4]$ was obtained from Fluka and purified according to the literature procedure.[36a] Triply distilled water was used to prepare all solutions. The final concentration of C-153 in all experiments was kept at 5×10^{-6} M. All experiments were carried out at 298 (±1) K. C-153 is initially dissolved in methanol and transfer to a vial. Then water is added to the vial after removing the methanol under vacuum. Then the solution is transferred in the quartz cuvette for experiments.

The absorption and fluorescence spectra were measured using a Shimadzu (model no. UV-1601) spectrophotometer and a Spex-Fluorolog-3 (model no. FL3-11) spectrofluorimeter. The fluorescence spectra were corrected for the spectral sensitivity of the instrument. For steady-state experiments, all samples were excited at 408 nm. The setup for time-resolved fluorescence measurements was described in detail in our earlier publication.[26] Briefly, the samples were excited at 408 nm using a picosecond diode laser (IBH), and the signals were collected at magic angle (54.7°) polarization using a Hamamatsu microchannel plate photomultiplier tube (3809U). The instrument response function of our setup is ~90 ps. The same setup was used for anisotropy measurements. For the anisotropy decays, we used a motorized polarizer in the emission side. The emission intensities at parallel ($I_{||}$) and perpendicular ($I_{\perp}$) polarizations were collected alternatively until a certain peak difference between parallel ($I_{||}$) and perpendicular ($I_{\perp}$) decays were reached. The peak differences depended on the tail matching of the parallel ($I_{||}$) and perpendicular ($I_{\perp}$) decays. The analysis of the time-resolved data and anisotropy decays were done using IBH DAS, version 6, decay analysis software. All experiments were carried out at 298 K. The same software was also used to analyze the anisotropy data. For dynamic light scattering (DLS) measurements, we used a Malvern Nano ZS instrument employing a 4 mW He−Ne laser ($\lambda = 632.8$ nm) and equipped with a thermostated sample chamber. All experiments were carried out at 173° scattering angle at 298 K. For viscosity measurements, we used an advanced rheometer (TA instrument, AR 1000) at 298 K.

(31) Fletcher, K. A.; Pandey, S. *Langmuir* **2004**, *20*, 33.
(32) (a) Gao, H.; Li, J.; Han, B.; Chen, W.; Zhang, J.; Zhang, R.; Yan, D. *Phys. Chem. Chem. Phys.* **2004**, *6*, 2914. (b) Cheng, S.; Zhnag, J.; Zhang, Z.; Han, B. *Chem. Comm.* **2007**, 2497.
(33) Gao, Y.; Han, S.; Han, B.; Li, G.; Shen, D.; Li, Z.; Du, J.; Hou, W.; Zhang, G. *Langmuir* **2005**, *21*, 5681.
(34) Eastoe, J.; Gold, S.; Rogers, S. E.; Paul, A.; Welton, T.; Heenan, R. K.; Grillo, I. *J. Am. Chem. Soc.* **2005**, *127*, 7302.
(35) Patrascu, C.; Gauffre, F.; Nallet, F.; Bordes, R.; Oberdisse, J.; de Lauth-Viguerie, N.; Mingotaud, C. *Chem. Phys. Chem.* **2006**, *7*, 99.
(36) (a) Miskolczy, Z.; Sebok-Nagy, K.; Biczok, L.; Gökturk, S. *Chem. Phys. Lett.* **2004**, *400*, 296. (b) Blesic, M.; Marques, M. H.; Plechkova, N. V.; Seddon, K. R.; Rebelo, L. P. N.; Lopes, A. *Green Chem.* **2007**, *9*, 481. (c) Modaressi, A.; Sifaoui, H.; Mielcarz, M.; Domanska, U.; Rogalski, M. *Colloids Surf. A* **2007**, *302*, 181. (d) Bowers, J.; Butts, C. P.; Martin, P. J.; Vergara-Gutierrez, M. C.; Heenan, R. K. *Langmuir* **2004**, *20*, 2191. (e) Baker, G. A.; Pandey, S.; Pandey, S.; Baker, S. N. *Analyst* **2004**, *129*, 890. (f) Schnee, V. P.; Baker, G. A.; Rauk, E.; Palmer, C. P. *Electrophoresis* **2006**, *27*, 4141. (g) Wang, J.; Wang, H.; Zhang, S.; Zhang, H.; Zhao, Y. *J. Phys. Chem. B* **2007**, *111*, 6181. (h) Singh, T.; Kumar, A. *J. Phys. Chem. B* **2007**, *111*, 7843. (i) Goodchild, I.; Collier, L.; Millar, S. L.; Prokes, I.; Lord, J. C. D.; Butts, C. P.; Bowers, J.; Webster, J. R. P.; Heenan, R. K. *J. Colloids Interface Sci.* **2007**, *307*, 455. (j) Vanyur, R.; Biczok, L.; Miskolczy, Z. *Colloids Surf. A* **2007**, *299*, 256. (k) Dong, B.; Zhang, J.; Zheng, L.; Wang, S.; Li, X.; Inoue, T. *J. Colloids Interface Sci.* **2008**, *319*, 338.
(37) (a) Wasserscheid, P.; Hal, R. V.; Bösmann, A. *Green Chem.* **2002**, *4*, 400. (b) Davila, M. J.; Aparicio, S.; Alcalde, R.; Garcia, B.; Leal, J. M. *Green Chem.* **2007**, *9*, 221.
(38) Dattelbaum, A. M.; Baker, S. N.; Baker, G. A. *Chem. Commun.* **2005**, 939.
(39) Maroncelli, M.; Fleming, G. R. *J. Chem. Phys.* **1987**, *86*, 6221.
(40) (a) Jones, G., II; Jackson, W. R.; Choi, C.-Y.; Bergmark, W. R. *J. Phys. Chem.* **1985**, *89*, 294. (b) Rechthaler, K.; Köhler, G. *Chem. Phys.* **1994**, *189*, 99.
(41) (a) Chakraborty, A.; Seth, D.; Setua, P.; Sarkar, N. J. *Chem. Phys.* **2006**, *124*, 074512. (b) Chakraborty, A.; Seth, D.; Setua, P.; Sarkar, N. *J. Phys. Chem. B* **2006**, *110*, 16607.
(42) (a) Sarkar, N.; Datta, A.; Das, S.; Bhattacharyya, K. *J. Phys. Chem.* **1996**, *100*, 15483. (b) Nandi, N.; Bhattacharyya, K.; Bagchi, B. *Chem. Rev. (Washington, D. C.* **2000**, *100*, 2013. (c) Bagchi, B. *Chem. Rev.* **2005**, *105*, 3197.
(43) Hazra, P.; Chakrabarty, D.; Chakraborty, A.; Sarkar, N. *Biochem. Biophys. Res. Commun.* **2004**, *314*, 543.
(44) Quitevis, F. L.; Marcus, A. H.; Fayer, M. D. *J. Phys. Chem.* **1993**, *97*, 5762.
(45) Maiti, N. C.; Krishna, M. M. G.; Britto, P. J.; Periasamy, N. *J. Phys. Chem. B* **1997**, *101*, 11051.
(46) Dutt, G. B. *J. Phys. Chem. B* **2003**, *107*, 10546.
(47) Nandi, N.; Bagchi, B. *J. Phys. Chem. B* **1997**, *101*, 10954.
(48) Nandi, N.; Bagchi, B. *J. Phys. Chem. A* **1998**, *102*, 8217.

Table 1. Absorption, Emission Spectra, Stokes' Shift and Lifetime of C-153 in [C_4mim][C_8SO_4] Micelles

system	λ_{max}^{abs} (nm)	λ_{max}^{flu} (nm)	Stokes' shift ($\Delta\nu$, cm^{-1})	λ (cm^{-1})	$\langle\tau\rangle$ (ns)	viscosity (cP)
C-153 in water	434	550	5070	2990	1.70 (±0.03)	0.852
C-153 in [C_4mim][C_8SO_4] micelle at 0.5cmc	430	546	4940	2880	1.76 (±0.03)	0.892
C-153 in [C_4mim][C_8SO_4] micelle at cmc	430	543	4840	2770	2.00 (±0.03)	0.895
C-153 in [C_4mim][C_8SO_4] micelle at 5cmc	430	540	4740	2660	3.26 (±0.03)	0.965
C-153 in [C_4mim][C_8SO_4] micelle at 10cmc	426	540	4740	2660	3.28 (±0.03)	1.112

3. Results

3.1. Steady State Results. In water, the absorption peak of C-153 is at 434 nm. In [C_4mim][C_8SO_4]−water micelles at 5 and 10 times the cmc the respective absorption peak of C-153 was observed at 430 and 426 nm, respectively (Table 1). The absorption peak of C-153 in micelles was determined by subtracting the absorption spectra of C-153 in micelles from the respective absorption spectra of micelles without probes. This subtracted absorption spectra of C-153 in micelle is shown in Figure 1a. The emission peak of C-153 in [C_4mim][C_8SO_4]−water micelles at 5 and 10 times the cmc is at 540 nm. The emission spectra of C-153 in [C_4mim][C_8SO_4]−water micelles is shown in Figure 1b. The absorption and emission spectra of [C_4mim][C_8SO_4]−water micelles at 10 times the cmc without C-153 is shown in Figure 1. The contribution of fluorescence emission obtain from [C_4mim][C_8SO_4]−water micelles at 10 times the cmc is only ~5% compare to emission of C-153 in [C_4mim][C_8SO_4]−water micelles at 10 times the cmc at 540 nm, which is shown in Figure 1b.

3.2. Time-Resolved Studies. *3.2.1. Solvation Dynamics.* We have observed a dynamic Stokes' shift in the emission spectra of C-153 in both micelles. In micelles, the fluorescence transient of C-153 is dependent on the emission wavelength. At the red edge of the emission spectra, we have observed a decay profile that consists of a clear rise followed by usual decay, and at the blue end of the emission, a faster decay is observed, which is shown in Figure 2. All decay profiles were best fitted by a triexponential function. The time-resolved emission spectra (TRES) were constructed using the procedure of Fleming and Maroncelli.[39] The TRES at a given time t, $S(\lambda;t)$, is obtained by the fitted decays $D(t;\lambda)$, by relative normalization to the steady state spectrum $S_0(\lambda)$, as follows

$$S(\lambda;t) = D(t;\lambda)\frac{S_0(\lambda)}{\int_0^\infty D(t;\lambda)\,\mathrm{d}t} \tag{1}$$

Each time-resolved emission spectrum was fitted by the "log-normal line shape function", which is defined as

$$g(\nu) = g_0 \exp\left[-\ln 2\left(\frac{\ln[1+2b(\nu-\nu_p)/\Delta]}{b}\right)^2\right] \tag{2}$$

where g_0, b, ν_p, and Δ are the peak height, asymmetric parameter, peak frequency, and width parameter, respectively. A representative TRES of C-153 in [C_4mim][C_8SO_4]−water micelle at 10 times the cmc is shown in Figure 3. The peak frequency

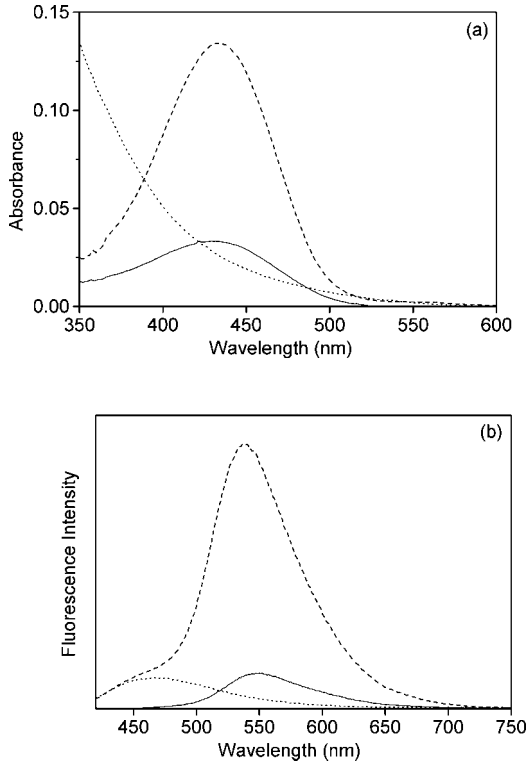

Figure 1. (a) Absorption spectra of C-153 in water (solid line), C-153 in [C_4mim][C_8SO_4] micelle at 10 times the cmc (dash line), and [C_4mim][C_8SO_4] micelle at 10 times the cmc without C-153 (dot line). (b) Emission spectra of C-153 in water (solid line), C-153 in [C_4mim][C_8SO_4] micelle at 10 times the cmc (dash line), and [C_4mim][C_8SO_4] micelle at 10 times the cmc without C-153 (dot line).

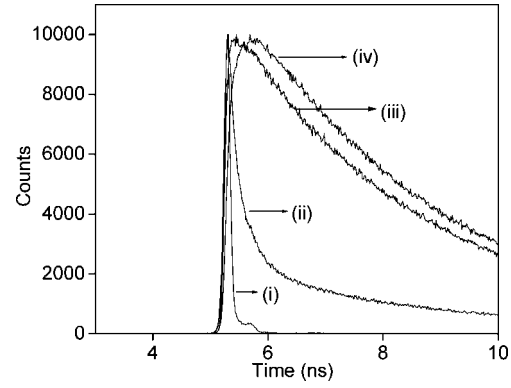

Figure 2. Fluorescence decay of C-153 in [C_4mim][C_8SO_4] micelle at 10 times the cmc at (i) instrument response function, (ii) 480 nm, (iii) 540, and (iv) 620 nm.

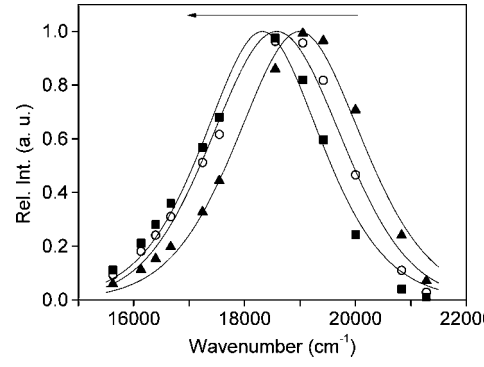

Figure 3. Time-resolved emission spectra (TRES) of C-153 in [C_4mim][C_8SO_4] micelle at 10 times the cmc at (i) 0 (▲), (ii) 200 (○), and (iii) 1000 (■) ps.

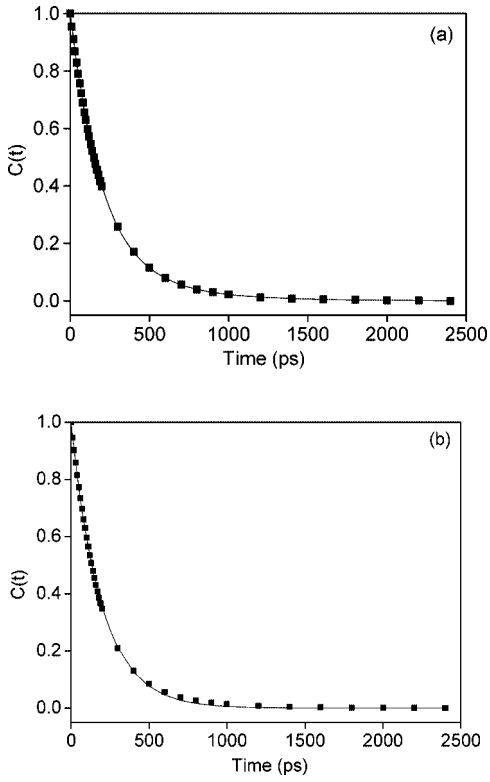

Figure 4. (a) Decay of solvent correlation function C(t) of C-153 in [C_4mim][C_8SO_4] micelle at 10 times the cmc. (b) Stretched exponential fit of C(t) of C-153 in [C_4mim][C_8SO_4] micelle at 10 times the cmc.

obtained from this log-normal fitting of TRES was then used to construct the decay of solvent correlation function [$C(t)$], which is defined as

$$C(t) = \frac{\nu(t) - \nu(\infty)}{\nu(0) - \nu(\infty)} \tag{3}$$

where $\nu(0)$ is the peak frequency at time $t = 0$ when electronic excitation occurs and $\nu(t)$ is the peak frequency at time $t = t$. $\nu(\infty)$ is the peak frequency at time $t = \infty$ when solvent molecule is in an equilibrium position around the photoexcited probe molecule. The decay of $C(t)$ with time was fitted to a biexponential function (Figure 4)

$$C(t) = a_1 e^{-t/\tau_1} + a_2 e^{-t/\tau_2} \tag{4}$$

where τ_1 and τ_2 are the two solvation times with amplitudes of a_1 and a_2, respectively. The decay parameters of $C(t)$ are summarized in Table 2. We observed a bimodal solvation time in both micelles. We also fitted $C(t)$ by a stretched exponential function

$$C(t) = \exp(-(t/\tau_0)^{\beta}) \tag{5}$$

where $0 < \beta \leq 1$, and the average solvation time is calculated by

$$\langle \tau_{solv} \rangle = \frac{\tau_0}{\beta} \Gamma(\beta^{-1}) \tag{6}$$

where Γ is the gamma function. The stretched exponential fitting parameters are tabulated in Table 3 and shown in Figure 4b. The average solvation times of C-153 in both micelles are almost same.

Table 3. Stretched Exponential Fitting Parameter of $C(t)$ of C-153 in [C_4mim][C_8SO_4]

system	τ_0 (ps)	β_{solv}	$\langle \tau_{solv} \rangle$ (ps)
C-153 in [C_4mim][C_8SO_4] micelle at 5cmc	189	0.94	194
C-153 in [C_4mim][C_8SO_4] micelle at 10cmc	192	0.99	193

3.2.2. Time-Resolved Anisotropy Studies. To get a better understanding of the microenvironment of C-153 in a micelle, time-resolved fluorescence anisotropy experiments were carried out. Time resolved fluorescence anisotropy [$r(t)$] is calculated using the following equation

$$r(t) = \frac{I_{||}(t) - GI_{\perp}(t)}{I_{||}(t) + 2GI_{\perp}(t)} \tag{7}$$

where G is the correction factor for detector sensitivity to the polarization direction of the emission. The G factor for our setup is 0.6. $I_{||}$ and $I_{\perp}$ are the fluorescence decays polarized parallel and perpendicular to the polarization of the excitation light, respectively. The anisotropy decay parameters of C-153 in both micelles are listed in Table 4 and shown in Figure 5. The rotational relaxation time of C-153 in water is 100 ps, whereas in both micelles the average rotational relaxation time of C-153 is 420 ps, i.e. the rotation of C-153 is hindered in micelles compared to neat water.

3.3. Dynamic Light Scattering (DLS) Measurements. We have measured the hydrodynamic diameter (D_h) of [C_4mim][C_8SO_4]−water micelles. A typical size distribution graph from the DLS experiment is shown in Figure 6. The average hydrodynamic diameter (D_h) of [C_4mim][C_8SO_4]−water micelles is 2.8 (±0.2) nm.

3.4. Viscosity Measurement. We also measured the viscosity of different ionic liquid micellar solutions. With gradual addition of [C_4mim][C_8SO_4] in water the bulk viscosity of the solutions gradually increases (Table 1).

4. Discussion

The emission peak of C-153 is blue-shifted compare to that of water in the [C_4mim][C_8SO_4]−water micelle. The emission peak of C-153 in the micelle is close to the emission peak of C-153 in 50% ethanol and 2,2,2-trifluoroethanol.[40] From this comparison, we can say that the polarity sensed by the C-153 molecule in micelles is less compared to neat water and is very close to the polarity of 50% ethanol or 2,2,2-trifluoroethanol. The emission peak of C-153 in these [C_4mim][C_8SO_4]−water micelles was very close to the emission peak of C-153 in dodecyltrimethylammonium bromide (DTAB) and sodium dodecyl sulfate (SDS) micelles.[41] Therefore, the micropolarity sensed by the C-153 molecules in [C_4mim][C_8SO_4] micelles is very similar to those of DTAB and SDS micelles. The emission peak of C-153 in [C_4mim][C_8SO_4]−water micelles is independent of the excitation wavelength. So all coumarin molecules feel similar environment inside the micelle. In water, the emission quantum yield of C-153 is ~0.12.[40a] In [C_4mim][C_8SO_4]−water micelle at 5 and 10 times the cmc, the emission quantum yields are 0.18 and 0.21, respectively. Moreover, with the addition of

Table 2. Decay Parameters of $C(t)$ for C-153 in [C_4mim][C_8SO_4] Micelles

system	$\Delta\nu^a$ (cm^{-1})	a_1	a_2	τ_1 (ns)	τ_2 (ns)	$\langle \tau \rangle$ (ps)
C-153 in [C_4mim][C_8SO_4] micelle at 5cmc	750	0.92	0.08	0.200	0.560	230 (±10)
C-153 in [C_4mim][C_8SO_4] micelle at 10cmc	700	0.85	0.15	0.200	0.505	245 (±10)

[a] $\Delta\nu = \nu_0 - \nu_\infty$.

Table 4. Rotational Relaxation Parameters of C-153 in [C4mim][C8SO4] Micelles

system	r_0	a_{1r}	τ_{1r} (ns)	a_{2r}	τ_{2r} (ns)	$\langle\tau_r\rangle^a$ (ns)
C-153 in water	0.40	1	0.100			0.100 (±0.005)
C-153 in [C_4mim][C_8SO_4] micelle at 0.5cmc	0.38	1	0.120			0.120 (±0.005)
C-153 in [C_4mim][C_8SO_4] micelle at cmc	0.38	1	0.145			0.145 (±0.005)
C-153 in [C_4mim][C_8SO_4] micelle at 5 cmc	0.39	0.40	0.760	0.60	0.190	0.420 (±0.01)
C-153 in [C_4mim][C_8SO_4] micelle at 10cmc	0.39	0.41	0.775	0.59	0.165	0.415 (±0.01)

[C_4mim][C_8SO_4] in water, the fluorescence Stokes' shifts become smaller, but after micelle formation, it becomes steady. The fluorescence Stokes' shifts remain unchanged at 5 and 10 times the cmc. The average fluorescence lifetime of C-153 in water is 1.70 ns, whereas in [C_4mim][C_8SO_4]−water micelle at 5 and 10 times the cmc the average lifetime of C-153 becomes 3.2 ns. Both steady state and time-resolved data indicated that C-153 is located in more hydrophobic and less polar region in micelles compared to water, and after formation of [C_4mim][C_8SO_4] micelles, the location of C-153 remains unchanged. The location of C-153 is probably in the Stern layer of the ionic liquid micelle.[42]

The solvent reorganization energy (λ) can be estimated from the steady-state spectra[59]

$$\lambda = \frac{\int_0^\infty \omega[\sigma_a(\omega) - \sigma_f(\omega)]\, d\omega}{\int_0^\infty [\sigma_a(\omega) + \sigma_f(\omega)]\, d\omega} \quad (8)$$

where $\sigma_a(\omega)$ and $\sigma_f(\omega)$ are the absorption and fluorescence maximum. The values of λ are tabulated in Table 1. This gradual change in Stokes' shift or λ up to the cmc is due to the increase in size of the aggregates with the increase in concentration of the RTIL. The probe molecules feel this change in environment until the cmc is reached. After the cmc is reached, the fluorescence Stokes' shift becomes unchanged, since there is no further change in the size of the micelles. The change in fluorescence Stokes' shift with the change in RTIL concentration is shown in Figure 7.

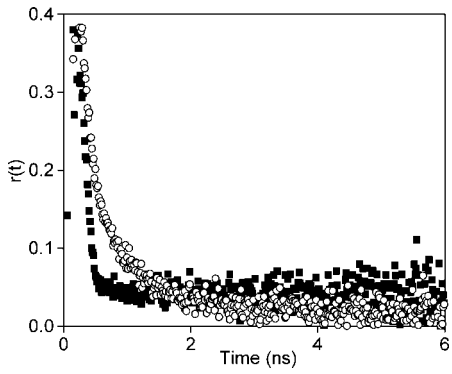

Figure 5. Decay of the time-resolved fluorescence anisotropy [$r(t)$] of C-153 in (i) water (■) and (ii) [C_4mim][C_8SO_4] micelles at 10 times the cmc (○).

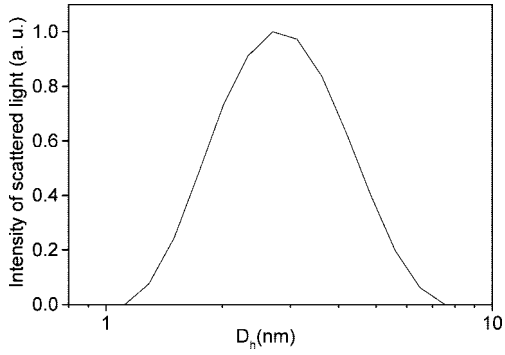

Figure 6. The size distribution graph for [C_4mim][C_8SO_4] micelles in water.

The rotational relaxation time [$r(t)$] of C-153 in water is 100 ps.[43] With a gradual increase in concentration of [C_4mim][C_8SO_4] in water, the rotational relaxation time gradually increases. Although increase in rotational relaxation time is not significant up to the cmc, after that it gradually increases, and at 5 and 10 times the cmc, the rotational relaxation time of C-153 becomes 420 ps. It suggests that the rotation of C-153 becomes more hindered after formation of the micelle (Figure 5). In neat water, the anisotropy decay of C-153 is single exponential. With an increase in RTIL concentration the anisotropy decay becomes bimodal and the percentage of slow component increases. Due to the formation of micelle, C-153 became more restricted in this micelle composed of an RTIL.

We have calculated several rotational parameters using two-step and wobbling in a cone models.[44–46] The biexponential nature of rotational relaxation decay in micelles is neither due to two different locations of probe molecule in the micelle nor due to the anisotropic rotation of the probe. The observed biexponential nature of rotational relaxation is due to the different types of rotational motion of probe molecules in the micelle. These different types of motion of probes are explained by the two-step model. The two-step model describes the fact that observed slow rotational relaxation is a convolution of the relaxation time corresponding to the overall rotation of the micelles (τ_m) and lateral diffusion of the monomers in the micelle (τ_D). The wobbling in a cone model describes the internal motion of the probe (τ_e) in terms of cone angle (θ_0) and wobbling diffusion coefficient (D_W). These parameters are obtained by the following equations

$$\frac{1}{\tau_1} = \frac{1}{\tau_e} + \frac{1}{\tau_2} \quad (9)$$

$$\frac{1}{\tau_2} = \frac{1}{\tau_D} + \frac{1}{\tau_m} \quad (10)$$

where τ_1 and τ_2 are the observed fast and slow components. The overall rotation of the micelle (τ_m) can be estimated using the Debye−Stokes−Einstein (DSE) relation

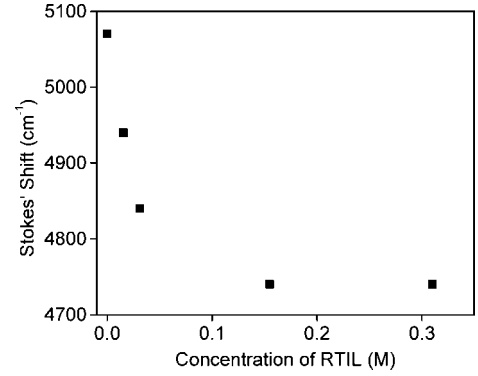

Figure 7. The variation of fluorescence Stokes' shift with change in RTIL concentration.

$$\tau_m = \frac{4\pi\eta r_h^3}{3kT} \quad (11)$$

where η is the viscosity of water. r_h is the hydrodynamic radius of the micelles, and k and T are the Boltzmann constant and absolute temperature, respectively. The hydrodynamic radius of $[C_4mim][C_8SO_4]$ micelle in water is observed as 1.4 nm, which is determined from the DLS measurement. The lateral diffusion constant is defined as

$$D_L = \frac{r_h^2}{6\tau_D} \quad (12)$$

We have calculated the order parameters (S) from the following equation to know the exact location of the probe.

$$S^2 = a_{2r} \quad (13)$$

The magnitude of the S is a measure of spatial restriction and has values from zero (unrestricted motion) to 1 (completely restricted motions). The value of S in this micelle is 0.64. We have calculated the cone angle θ_0 and wobbling diffusion coefficient as follows

$$\theta_0 = \cos^{-1}\left[\frac{1}{2}((1+8S)^{1/2}-1)\right] \quad (14)$$

$$D_w = \frac{7\theta^2}{24\tau_e} \quad (15)$$

where θ_0 is the cone angle in radians. The results of all these above analytical parameters are tabulated in Table 5.

The average solvation time of C-153 is almost remaining unchanged with $[C_4mim][C_8SO_4]$ concentration. Although the notable point is that with an increase in $[C_4mim][C_8SO_4]$ concentration the weightage of the slow component is increasing. The observed dynamics is bimodal in both micelles. Nandi and Bagchi proposed "dynamics exchange" between free and bound water molecules, which is responsible for the bimodal dynamics of solvation in the micelle.[47,48] The water molecules, counterions, and polar head groups of surfactants are responsible for solvation in micelle. Recent computer simulation studies showed that hydrogen bonding between water molecules and polar head groups of the surfactant are much stronger than the hydrogen bond between two water molecules.[49–52] These two types of water molecules are responsible for the slow and fast component of solvation dynamics. Both the faster and slower time constants of solvent relaxation remain unchanged with an increase in $[C_4mim][C_8SO_4]$ concentration. The average solvation time also remain unchanged with an increase in $[C_4mim][C_8SO_4]$ concentration. The similar type of observation that solvation time remain unchanged with an increase in surfactant concentration was already noticed by Shirota et al.[53] With an increase in RTIL concentration, the density of the micelle, i.e., number of micelles in water increases, which eventually increases the amplitude of the slow component with an increase in RTIL concentration. Moreover, an interesting point to be noted is that the solvation dynamics in this $[C_4mim][C_8SO_4]$ micelle is faster than the solvation dynamics in $C_8H_{17}SO_4Na$ micelle reported by Tamoto et al.[54] This is occurring probably due to the replacement of Na^+ ion by $[C_4mim]^+$. The relatively slow solvation dynamics in the

Table 5. Analytical Rotational Parameters of C-153 in $[C_4mim][C_8SO_4]$ Micelles

τ_m (ns)	τ_e (ns)	τ_D (ns)	$D_w \times 10^{-8}$ (s^{-1})	$D_L \times 10^6$ (cm^2/s)	θ_0 (deg)	S
3.1	0.209	1.03	7.66	3.39	42.5	0.64

Stern layer of the $C_8H_{17}SO_4Na$ micelle is due to the motion of the Na^+ ions and the water molecules confined in the micellar cavity. The interaction of the Na^+ ions with the headgroup of the micelle is also responsible for the slow dynamics. Chakrabarty et al.[55] showed that the solvation dynamics in Triton X-100 (TX-100)−bile salt (sodium deoxycholate, NaDC) containing mixed micelles is faster than the solvation dynamics in NaDC micelles due to the removal of Na^+ ion from the Stern layer. The solvation dynamics becomes fast in mixed micelles. In the present study, we have also observed similar behavior in that the replacement of Na^+ ion by $[C_4mim]^+$ results faster dynamics. The mobility of the $[C_4mim]^+$ ions is slow, because the chain dynamics is quite slow.[56] The solvent relaxation in an ionic liquid surfactant is different from that in a conventional ionic surfactant. The slow component of the solvation dynamics in $C_8H_{17}SO_4Na$ micelle is on the nanoseconds time scale,[54] whereas in $[C_4mim][C_8SO_4]$ micelle the same component is on the subnanoseconds time scale. It is reported that, with an increase in alkyl chain length, solvation time increases.[54] Due to this reason, solvation dynamics in the present system is much faster than the solvation dynamics in SDS micelles.[53] The anionic sulfate group directly forms hydrogen bonds with the water molecules.[54] These hydrogen bonds strongly influence the observed solvation dynamics in micellar solutions.

The solvation dynamics in neat $[C_4mim]^+$ ion containing RTILs are well-studied.[9–22] The slowest solvation time in neat $[C_4mim]$ RTILs are a few nanoseconds, which are much slower compared to the present micellar system. It indicates that the hydration of water contributes largely to the solvation dynamics in the present system.

In the present study, using the time correlated single photon counting (TCSPC) setup, we are missing the fast components of the solvation dynamics (<90 ps). We can apply the method of Fee and Maroncelli[57] to calculate the missing component. We have calculated the time zero spectrum using the above procedure. The time zero frequency can be estimated using the following relation

$$\nu_{p,md}(t=0) \approx \nu_{p,md}(abs) - [\nu_{np,md}(abs) - \nu_{np,md}(em)] \quad (16)$$

where the subscripts p and np refer to the polar and nonpolar spectrum, respectively, and the frequencies here are not the values at maxima but corresponds to the midpoint frequencies, ν_{md}, in the solvent. The missing component is $[\nu_{cal}(0) - \nu(0)]/[\nu_{cal}(0) - \nu(\infty)]$. Using the above procedure, we have calculated that we are missing ~57% of the total dynamics in both micelle using C-153 as our experimental probe. One of the interesting observations of the present work is that the missing component of the solvation dynamics of $[C_4mim][C_8SO_4]$ micelles is smaller than that of $C_8H_{17}SO_4Na$ micelles, while the solvation time of $[C_4mim][C_8SO_4]$ micelles is faster than that of $C_8H_{17}SO_4Na$ micelles.[54] The different molecular motion, reorientation, and translation with different time scale in these two systems are the reason behind this observation. Moreover, the nature of interaction between water and the cations and anions of RTIL is different

(49) Balasubramanian, S.; Bagchi, B. *J. Phys. Chem. B* **2001**, *105*, 12529.
(50) Balasubramanian, S.; Pal, S.; Bagchi, B. *Phys. Rev. Lett.* **2002**, *89*, 115505.
(51) Pal, S.; Balasubramanian, S.; Bagchi, B. *J. Chem. Phys.* **2002**, *117*, 2852.
(52) Pal, S.; Balasubramanian, S.; Bagchi, B. *J. Phys. Chem. B* **2003**, *107*, 5194.
(53) Shirota, H.; Tamoto, Y.; Segawa, H. *J. Phys. Chem. A* **2004**, *108*, 3244.
(54) Tamoto, Y.; Segawa, H.; Shirota, H. *Langmuir* **2005**, *21*, 3757.
(55) Chakrabarty, D.; Hazra, P.; Sarkar, N. *J. Phys. Chem. A* **2003**, *107*, 5887.
(56) Cassol, R.; Ge, M.-T.; Ferrarini, A.; Freed, J. H. *J. Phys. Chem. B* **1997**, *101*, 8782.
(57) Fee, R. S.; Maroncelli, M. *Chem. Phys.* **1994**, *183*, 235.

from that of the cations and anions of ionic surfactant, which is reflected in this solvation dynamics results.

From the solvation dynamics study in RTIL micelle, it is revealed that the slow component of solvation dynamics is much faster compared to the conventional micelles. The average solvation time is also much smaller compared to conventional micelles. It is well-known that the micelles have widespread use in extraction, synthesis, and purification and the solvation is a key step to control all these processes. As the solvation dynamics in this micelle composed of an RTIL is widely different from conventional micelles, these results will definitely be helpful to understand the behavior of these RTIL micelles for practical use.

5. Conclusion

1-Butyl-3-methylimidazolium octyl sulfate aggregates in water to form micelles.[36a] The diameter of this novel RTIL-containing micelle is ~2.8 (±0.2) nm. The solvent and rotational relaxations in these micelles were investigated by picosecond time-resolved fluorescence spectroscopy using C-153 as a probe. Both the solvent and rotational relaxation of C-153 were hindered several times in this RTIL-containing micelle compared to the solvation time of a similar type of coumarin dye in bulk water.[58] The average solvation time in [C_4mim][C_8SO_4] micelles is relatively smaller compared to conventional micelles.[42,53,54] Most interestingly, the slow component of solvent relaxation in these [C_4mim][C_8SO_4] micelles is on the subnanoseconds time scale, whereas in other micelles such as $C_8H_{17}SO_4Na$ or TX-100 the same component is on the nanosecond time scale.[42a,53] Both the percentage missing component and solvent relaxation time indicate that the solvation dynamics in [C_4mim][C_8SO_4] micelles is different from that of conventional ionic micelles due to the different molecular motion, reorientation, and translation, with different time scale.

Acknowledgment. N.S. is thankful to the Department of Science and Technology (DST) and Council of Scientific and Industrial Research (CSIR), Government of India, for generous research grants. D.S. and S.S. are thankful to CSIR for research fellowships. The authors are thankful to Dr. S. K. Pal of S. N. Bose National Center for Basic Sciences, Kolkata, for user of the dynamic light scattering equipment.

Note Added After ASAP Publication. This article was published ASAP on June 14, 2008. Due to a production error, changes have been made to Table 1. The correct version was published on June 19, 2008.

LA800813U

(58) (a) Jimenez, R.; Fleming, G. R.; Kumar, P. V.; Maroncelli, M. *Nature* **1994**, *369*, 471. (b) Vajda, S.; Jimenez, R.; Rosenthal, S. J.; Fidler, V.; Fleming, G. R.; Castner, E. W., Jr. *J. Chem. Soc., Faraday Trans* **1995**, *91*, 867.

(59) Jordanides, X. J.; Lang, M. J.; Song, X.; Fleming, G. R. *J. Phys. Chem. B* **1999**, *103*, 7995.